

Modular Chemoenzymatic Synthesis of Ten Fusicoccane Diterpenoids

Authors: Yanlong Jiang,¹ Hans Renata^{1,*}

Affiliations:

¹Department of Chemistry, BioScience Research Collaborative, Rice University, Houston, TX, 77005, USA

*Corresponding author. Email: hrenata@rice.edu

Abstract: Fusicoccane diterpenoids display intriguing biological activities, including the ability to act as molecular glue modulators of 14-3-3 protein–protein interaction. However, their innate structural complexity and diverse oxygenation patterns present enormous synthetic challenges. Here, a modular chemoenzymatic approach to this natural product family that combines de novo skeletal construction and late-stage hybrid C–H oxidations is presented. A convergent fragment coupling strategy allowed rapid access to a key tricyclic intermediate, which was subjected to chemical and enzymatic C–H oxidations to modularly prepare five oxidized family members. Complementarily, a biomimetic skeletal remodeling was conceived to render five rearranged fusicoccanes with unusual bridgehead double bonds synthetically accessible for the first time.

One-Sentence Summary: Ten complex fusicoccane diterpenoids were synthesized by combining de novo skeletal construction and late-stage chemical and enzymatic C–H oxidations.

Main Text:

The fusicocanes are fungal diterpenoids that are defined by their 5/8/5 ring system (Figure 1A).¹ While the two flagship family members, cotylenin A (**1**) and fusicoccin A (**2**), are phytotoxins that target the 14-3-3 protein–protein interaction (PPI), additional family members also exhibit a diverse range of biological functions.^{2–6} Conserved across eukaryotes, the 14-3-3 proteins serve as adaptor proteins that regulate many cellular processes by binding to a variety of disease-relevant phosphoprotein clients, such as Raf kinases and the YAP transcriptional modulator.⁷ In line with its 14-3-3 modulatory activity, **1** is known to induce apoptosis and has been used in combination with anti-epidermal growth factor receptor antibody and kinase inhibitors to suppress tumor growth.^{4,8,9} Interestingly, the sugar moiety of **1** is not a key determinant for activity as cotylenol is moderately cytotoxic on human myeloid leukaemia cells¹⁰ and is also capable of serving as a molecular glue to form a ternary complex with 14-3-3 isoforms and their clients.¹¹ The unique biological activities of **1** and **2** have spurred a sustained research in the discovery of new family members, resulting in more than 50 fusicoccane-type terpenoids isolated to date, including some that contain rearranged skeletons (e.g., **4–6**).^{12–14} Additionally, there has been a widespread interest in developing semisynthetic derivatives of **1** and **2** as small molecule modulators of 14-3-3 PPIs, from which useful structure-activity relationship insights have emerged.^{15,16}

Despite their promising biological activities, access to the fusicocanes and their derivatives has been challenging as many family members can only be isolated in small quantities as a mixture of congeners. The native fungal producer of **1** and **3**, *Cladosporium* sp. 501-7W, has also lost its ability to proliferate during preservation.¹⁷ A number of total syntheses have been reported.^{18–23} However, they range between 15 and 29 steps in length, highlighting the synthetic challenges posed by these molecules, especially by the more oxidized members of the family. Importantly, a unified strategy that allows for a concise yet versatile access to a wide range of family members has not been demonstrated. Here we report an efficient, family-level synthetic solution to the C3-oxidized fusicoccane diterpenoids by employing a chemoenzymatic approach. Ten family members, namely cotylenol, brassicenes A, C, F, H, I, J, K, L and R were divergently synthesized in 8–13 steps each (longest linear sequence) from commercially available materials, (+)-limonene oxide and (–)-limonene, by going through a common synthetic intermediate. This work represents the shortest route to cotylenol to date and the first syntheses of all the aforementioned brassicenes. Notably, several rearranged fusicocanes with unusual bridgehead double bonds have also been made synthetically accessible for the first time with our strategy.

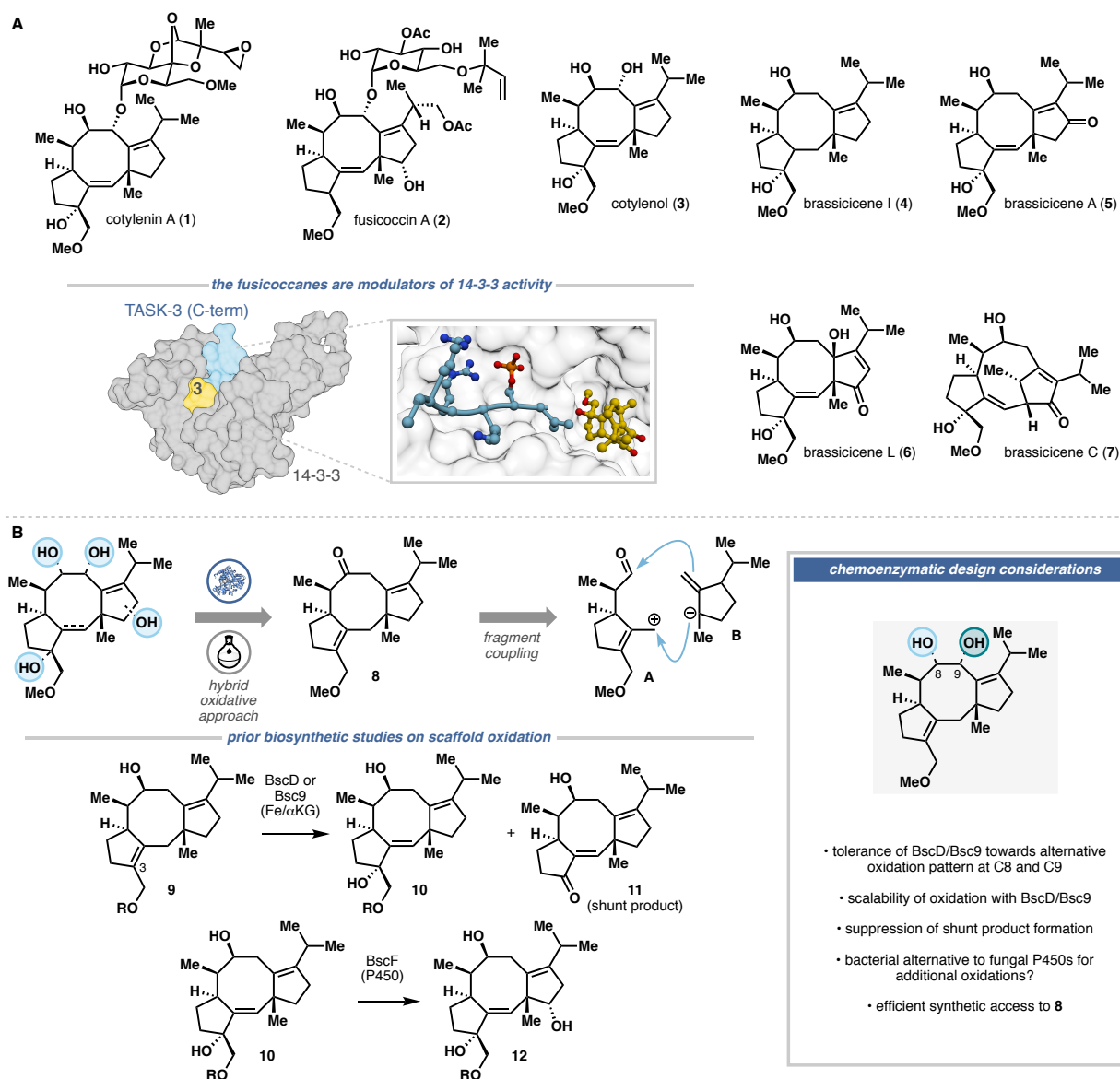


Figure 1. Fusicoccane diterpenoids and overview of current study. (A) Representative members of fusicoccane diterpenoid family and their biological activities. (B) Retrosynthetic strategy for accessing a diverse range of fusicoccanes by relying on late-stage hybrid oxidations and efficient skeletal construction.

A hybrid oxidative approach²⁴ by combining enzymatic and chemical C–H oxidations on a minimally-functionalized intermediate was adjudged to be the most versatile means to modularly access a wide range of fusicoccanes (Figure 1B). Distinct from our previous application of hybrid oxidative approach that centered on the semisynthetic modifications of pre-existing carbocycles, the current work relies on its synergy with skeletal construction events to achieve efficient total synthesis. Here, ketone **8** was targeted as the key point of divergence. This compound was envisioned to arise from synthons **A** and **B** through two C–C bond forming events, for which Takeshita’s allylation-based approach¹⁸ serves as a strategic inspiration due to its ability to construct the key quaternary center at C11 with high stereoselectivity. Prior independent studies by Dairi and Oikawa have identified the role of the non-heme dioxygenases (NHDs) BscD and

Bsc9 in the generation of the C3 alcohol.^{17,25} In the native biosynthetic pathway, alcohol **9** undergoes an initial hydrogen atom abstraction at C1, which leads to subsequent olefin isomerization and radical rebound at C3 to produce **10** along with shunt product **11**. While the extent of the shunt product formation and the catalytic efficiency of BscD and Bsc9 were unclear at the outset, the biocatalytic oxidation transform was deemed strategic and worth the risk, especially in light of the challenges involved in installing the C3 alcohol in prior syntheses. In a further departure from the native biosynthetic pathway, our synthetic design would also require the use of substrate(s) with alternative oxidation pattern at C8 and C9 relative to **9** for route brevity. This decision posed an added risk as the substrate promiscuity of the two enzymes have not been investigated. In addition to BscD and Bsc9, several P450s are involved in the oxidative tailoring of the scaffold in the native biosynthetic pathway.²⁵ However, the membrane-bound nature of these enzymes would likely limit their synthetic utility and we speculated that with sufficient screening, we would be able to identify bacterial P450s, which are known to display better biocatalytic utility,^{26,27} as alternative means to oxidize other remote positions on the 5/8/5 tricycle.

Fragment Synthesis and Assembly of Fusicoccane Core

Serving as a synthetic equivalent of **A**, cyclopentenol **16** was prepared in three steps from (+)-limonene oxide (**13**, Figure 2A). Though simplified variants of **16** have previously been prepared from limonene,²⁸ an efficient strategy to introduce the allylic methyl ether needed to be identified. Towards this goal, **13** was first subjected to a regioselective epoxide opening using a known literature procedure.²⁹ A telescoped protocol involving VO(acac)₂-catalyzed epoxidation, epoxide ring opening with NaOMe and oxidative cleavage with NaIO₄ furnished aldehyde **15**. Finally, an intramolecular aldol condensation completed the synthesis of **16**. This three-step sequence could be routinely conducted on decagram scale with satisfactory overall yield (55%). The intended coupling partner, allyl chloride **17** was prepared in three steps through slight modifications of a known route.^{22,28} Union of **16** and **17** was realized by employing Fürstner's modification of the Nozaki-Hiyama-Kishi (NHK) reaction.³⁰ This modification was chosen for both safety and strategic reasons as the catalytic use of low-valent chromium salt would minimize potential physiological hazards, and the use of TMSCl as the reaction mediator would allow for simultaneous capping of the C1 alcohol as the TMS ether. Selective hydroboration of the isopropenyl unit and subsequent oxidation to the aldehyde were combined in a telescoped protocol to afford **19**, whose stereochemical configuration was verified through single-crystal X-ray diffraction analysis of a related derivative (**S9**).

Submission of **19** to a Prins reaction in the presence of BF₃•Et₂O generated a 5/8/5 tricycle (**S10**) that contains all the necessary chemical handles for accessing **8**. At this stage, the extraneous hydroxyl group at C1 needed to be excised. During our attempts to deprotect the TMS group, the use of TFA on **S10** was found to effect deoxygenation at C1 along with the formation of a ketone moiety at C8 (ie. compound **8**). Furthermore, the C8 stereochemical configuration of **S10** is vital for this process as its corresponding C8-epimer was found incapable of undergoing the same deoxygenation. Though further studies are still needed, this unusual transformation likely proceeds through selective ionization of the C1 hydroxyl group, which initiates a transannular hydride transfer from the C8 carbon. Using this discovery as a starting point, we looked to identify a suitable protocol to convert **19** to **8** in one step. An extensive test of Lewis and Brønsted acids for this conversion eventually led to the development of a one-pot protocol featuring an initial treatment with BF₃•Et₂O, followed by the addition of tetra-*n*-butylammonium bifluoride

(TBABF), which likely reacts with BF_3 to generate HBF_4 in situ.³¹ In comparison, stronger conditions tested led to simple elimination of the C1-OH (see Table S4 in the Supporting Information). Prior syntheses of **3** had established the viability of installing the C9 hydroxyl group via enolate α -oxidation with MoOPH. Due to safety and toxicity issues associated with preparing MoOPH³² on large scale, an alternative set of conditions to effect this transformation was sought. A combination of LiOtBu and KH and molecular oxygen in the presence of $\text{P}(\text{OMe})_3$ was found to afford **20** in high conversion, selectivity and isolated yield, though a minor byproduct arising from α -oxidation at C7 could also be observed (see Table S5 in the Supporting Information). As a testament to the scalability of the route, the entire sequence toward **20** could be routinely conducted on gram-scale or near gram-scale to provide ample material supply for subsequent oxidative tailoring.

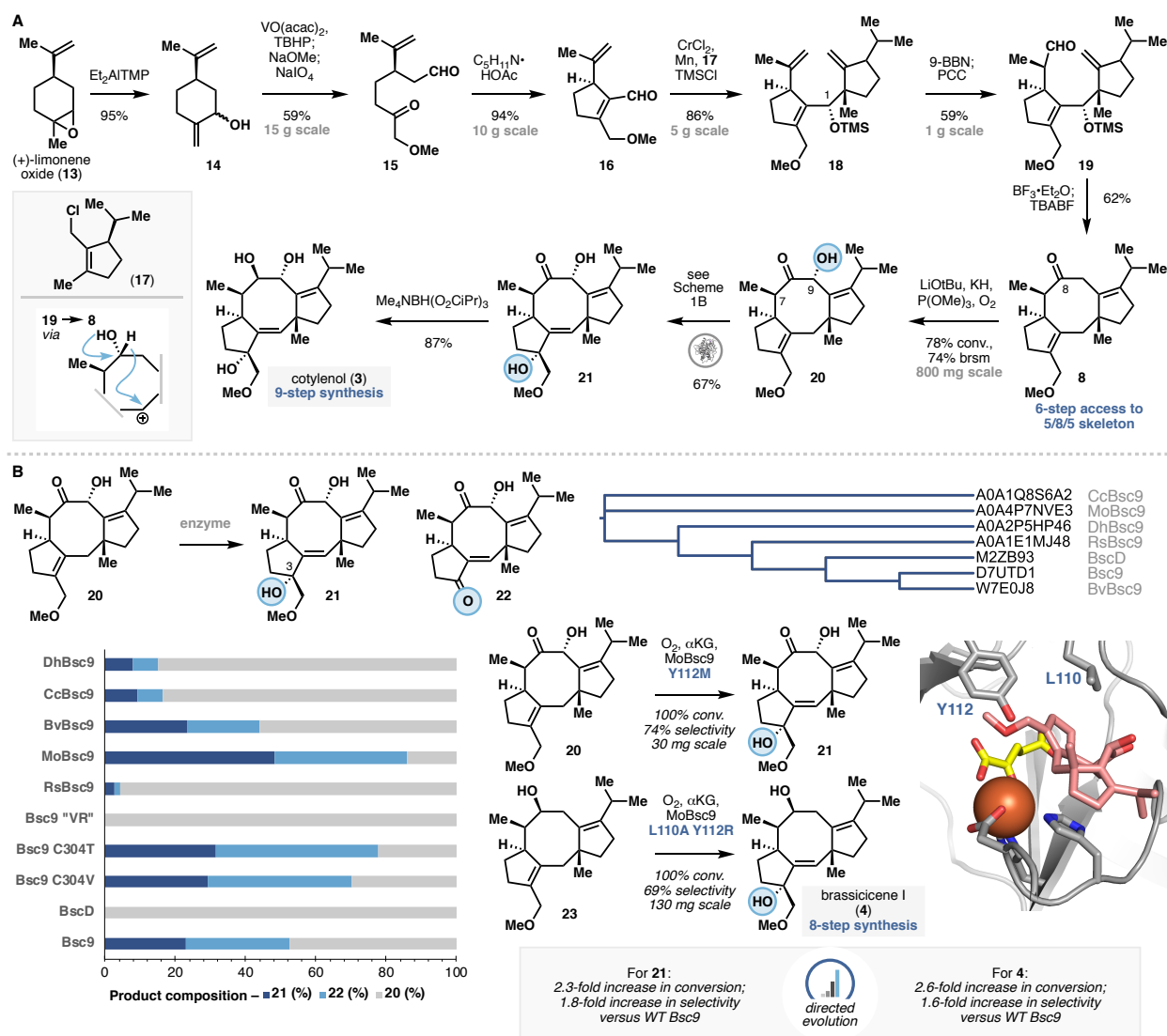


Figure 2. Assembly of the fusicoccane core and completion of the synthesis of cotylenol and brassicene I. (A) Fragment coupling approach to synthesize key intermediate **8** and its conversion to cotylenol. **(B)** Homolog screening and enzyme engineering to optimize site- and chemoselective oxidation at C3.

Enzymatic Tool Development and Synthesis of Cotylenol

Setting our sights on cotylenol, we investigated the biocatalytic use of BscD and Bsc9 for the oxidation of **20**. While Bsc9 could be heterologously expressed as a *N*-His₆-tagged protein in *E. coli*, BscD was found to be completely insoluble. BscD and Bsc9 share *ca.* 70% sequence identity, and the regions of divergence are primarily found in their *N*-terminal domains—in which Bsc9 contains an additional 26-residue sequence—and two insertion segments. Grafting of Bsc9's *N*-terminal domain onto BscD was attempted, but this effort did not lead to any improvement in soluble protein yield. Reaction of **20** with Bsc9 in cell lysates provided a mixture of the desired tertiary alcohol product (**21**) and shunt product **22** with moderate conversion (Figure 2B). In accordance, no reaction was observed with *E. coli* lysates containing BscD. In their initial discovery of Bsc9, Dairi and co-workers proposed that the shunt product arises from trapping of the tertiary radical at C3 with molecular oxygen through the intermediacy of a dioxetane species.¹⁷ As no further mechanistic studies were performed by Dairi and co-workers, we sought to investigate whether **22** could have arisen from **21** via enzyme-assisted oxidative cleavage. From the perspective of reaction optimization, we speculated that if **21** is actually derived from **22**, the ratio of **21:22** could be readily modulated by adjusting the reaction conditions. Subjecting **22** to the enzymatic transformation led to no reaction, disproving this hypothesis. Importantly, this observation suggested that optimization of the product composition in the reaction would have to be achieved through alternative means.

During our initial tests of Bsc9 in cell lysates, a large batch-to-batch variability of the reaction outcome was observed. Eventually, this issue was rectified by developing a consistent and rigorous lysis protocol and ensuring that the lysates were used immediately for reaction. Addition of TCEP to the lysate was also found to improve conversion. In line with this observation, purified Bsc9 readily formed precipitates, suggesting rapid denaturation. Bsc9 contains two cysteine residues, one of which (C304) is predicted by homology model³³ to be surface exposed. We speculated that this residue could be targeted for mutagenesis to enhance the reaction outcome. While mutations C304V and C304T in Bsc9 resulted in small improvements in conversion, the ratio of **21:22** did not improve. Our homology model also predicted that one of the insertion segments in Bsc9 (Ala103–Gly116, hereby referred to as “active-site insertion”) lies opposite of the His-His-Asp iron-binding triad in the active site. As this region might be implicated in substrate binding, we generated a Bsc9-BscD chimera by swapping the Ala103–Gly116 sequence of Bsc9 with the corresponding Val-Arg diad from BscD. This chimera (Bsc9 “VR”) provided no reaction on **20**, suggesting the importance of the active-site insertion segment for hydroxylation activity on **20**. These drawbacks prompted us to test additional homologs of Bsc9 that diverge at the *N*-terminal and the active-site insertion region. Ten homologs were identified by picking the top ten hits from Genome Neighborhood Diagram (GND) analysis³⁴ and five of the ten were arbitrarily chosen for further characterization. Gratifyingly, a homolog from *Magnaporthe oryzae* (MoBsc9, 54% sequence identity to Bsc9) displayed improved conversion and ratio of **21:22**, which translates to *ca.* two-fold improvement in assay yield of **21**. No terpene synthase encoding genes could be identified within the vicinity of *MoBsc9*, suggesting that this dioxygenase might be involved in the biosynthesis of an entirely different natural product scaffold. Though the native function of this enzyme is still unclear to date, our discovery highlights the power of homolog screening in the unbiased discovery of superior enzyme(s) for a target reaction.³⁵

A brief directed evolution campaign was conducted to further improve the ratio of **21:22** in the enzymatic reaction. Based on our homology model of MoBsc9, two hydrophobic residues in the putative active site, L110 and Y112, were targeted for site-saturation mutagenesis. Reetz's "22-c trick" approach³⁶ to reduce codon redundancy was employed in combination with a thin layer chromatography-based (TLC-based) screening strategy previously developed in our laboratory.³⁷ In this round of screening, we identified mutation Y112M that afforded 8% improvement in selectivity while maintaining the high reaction conversion. Concurrently, screening of the Y112X library for reaction with **23**, prepared via one-step reduction of **8**, yielded variant Y112R that produced brassicene I (**4**) with 67% conversion and 51% selectivity (defined as percent ratio of the desired product : total products). As a comparison, WT Bsc9 provided only 37% conversion and 43% selectivity in this reaction. Using these two single mutants as parents, another round of evolution was performed by randomly mutagenizing L110. While only marginal improvement (less than 5%) could be obtained in testing the Y112M L110X library on **20**, the Y112R L110X library yielded variant L110A that further improved the selectivity for the production of **4** by 18%. Overall, our directed evolution campaign allowed for 2.3-fold improvement in conversion and 1.8-fold improvement in selectivity for the production of **21** and 2.6-fold improvement in conversion and 1.6-fold improvement in selectivity for the production of **4** relative to WT Bsc9. Preparative scale biocatalytic reaction on 30–50 mg scale with MoBsc9 Y112M could be conducted to afford **21** in 67% isolated yield. A corresponding reaction on **23** with MoBsc9 L110A Y112R on 100 mg scale provided brassicene I (**4**) in 64% isolated yield. The final reduction to provide cotylenol proceeded uneventfully under Nakada's conditions,²⁰ completing the synthesis in 9 steps (longest linear sequence) from commercial materials. Additionally, we achieved the first synthesis of brassicene I in 8 steps.

Synthesis of Eight Additional Fusicoccanes

Towards the goal of effecting selective C–H hydroxylation at other positions on the 5/8/5 tricycle, a concurrent screening of additional enzymatic and chemical oxidations was performed. Eight different variants of P450_{BM3}, previously developed in our laboratory for the site-selective C–H oxidation of decalin-containing terpenoids,^{37–40} were tested with brassicene I, revealing the ability of variant MERO1 L75A to effect selective hydroxylation at C13 to the corresponding allylic alcohol in 78% yield without any observable regioisomers (Figure 3A). Among the chemical methods surveyed, SeO₂ and CrO₃ yielded a complex mixture of products but the use of palladium-catalyzed allylic oxidation⁴¹ led to the direct formation of brassicene A (**5**) in moderate yield, completing a nine-step synthesis of this natural product. Alternatively, this compound could also be obtained via MnO₂-mediated oxidation of **24**. Rubottom oxidation of **5**, achieved via enol ether formation, reaction with mCPBA and TBAF desilylation, afforded brassicene R (**25**) with a total step count of 10. The ability of MERO1 L75A to effect allylic oxidation at C13 without any over-oxidation paved the way for accessing alternative oxidation patterns through the intermediacy of the corresponding diene. Treatment of **24** with HCl effected a clean elimination to cyclopentadiene **26**, which was then subjected to ¹O₂ [4 + 2] cycloaddition and Kornblum-DeLaMare rearrangement to complete the first synthesis of brassicene L (**6**) in 12 steps.

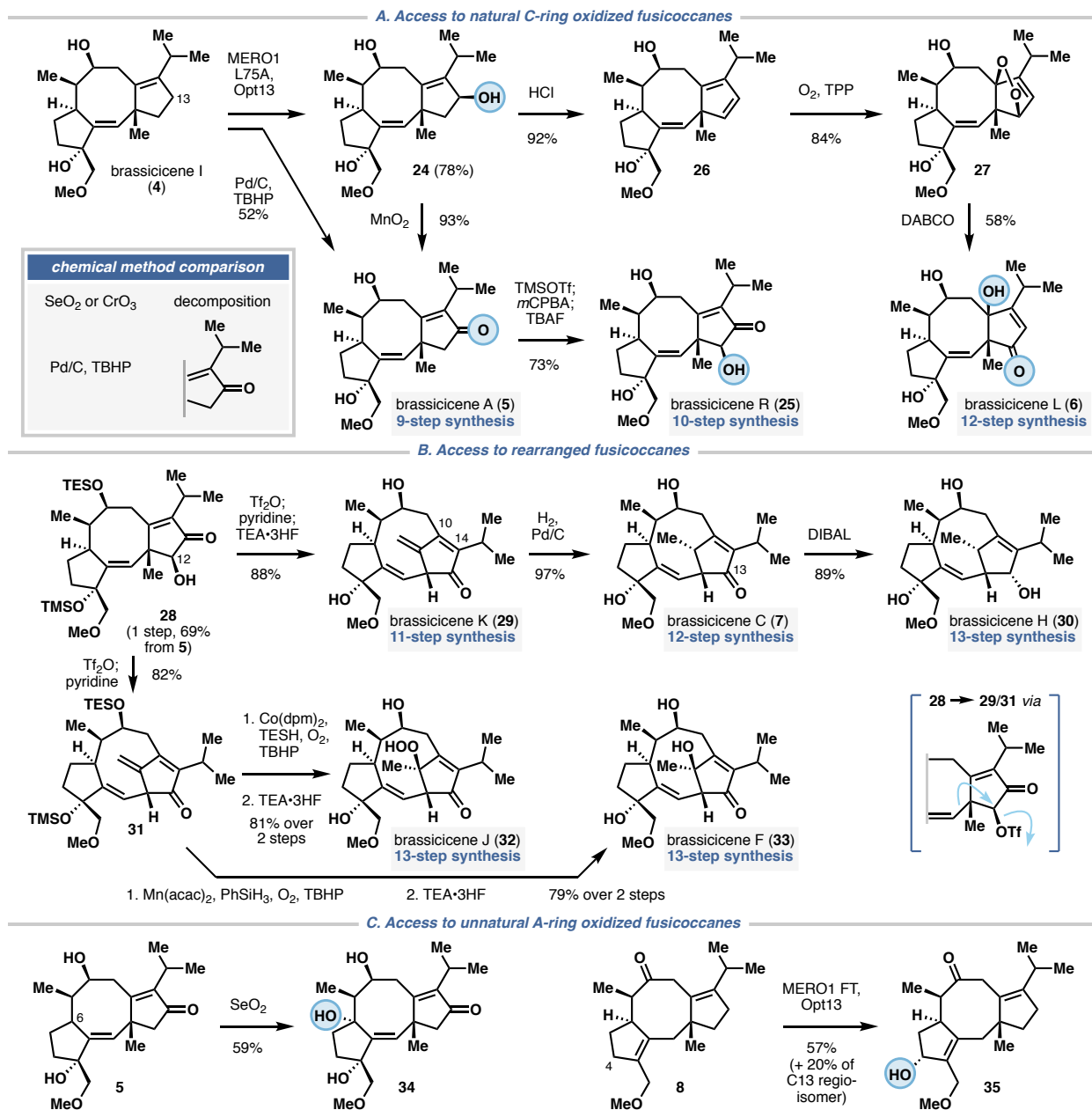


Figure 3. Completion of the synthesis of additional fusicoccenes. (A) C13 oxidation of 4 by P450_{BM3} variant MERO1 L75A and its application in the synthesis of brassicicenes A, L and R. (B) Synthesis of brassicicenes C, F, H, J and K through biomimetic skeletal rearrangement from 28. (C) Additional C–H oxidation results to synthesize unnatural fusicoccenes.

Ready access to 5 inspired us to design a biomimetic approach¹⁴ toward rearranged family members that share a common C10–C14 bridgehead double bond motif, such as brassicicenes C, H and K (Figure 3B). To date, compounds within this series have yet to succumb to synthetic efforts. Initial attempts to realize the rearrangement involved the direct functionalization of C12 with hypervalent iodine reagents,⁴² in the hope that the resulting iodinated species would spontaneously undergo a 1,2-rearrangement. However, this approach yielded no desired rearranged

product. After a similar failure with α -bromination at C12, **5** or its protected derivatives were examined as a suitable starting point for the proposed rearrangement. Gratifyingly, treatment of partially protected triol **28**, obtained from **5** in 1 step, with triflic anhydride followed by pyridine led to the spontaneous formation of a product with the desired rearranged skeleton, which was deprotected in the same pot to complete our synthesis of brassicene K (**29**) in 10 steps. Oikawa had originally proposed that the rearranged brassicenes could arise from either radical or carbocationic pathway and our result lent further support to the latter. The *exo*-methylene of **29** was chemo- and diastereoselectively reduced under hydrogenation conditions to furnish brassicene C (**7**). Finally, reduction of the C13 ketone of **7** afforded brassicene H (**30**), thereby completing the first synthesis of these three rearranged brassicenes. Though the autoxidation of **7** to brassicene J (**32**) was previously reported in the literature, the reaction proceeded with low conversion in our hands. The use of $^1\text{O}_2$ to drive the conversion was met with similarly disappointing results. As a workaround, protected brassicene K (**31**, accessible in one step from **28**) was subjected to Mukaiyama hydroperoxidation conditions,⁴³ followed by deprotection with $\text{Et}_3\text{N}\cdot 3\text{HF}$ to yield **32**. Attempts to effect this transformation in the absence of protecting group led to no reaction at all. Adjusting the metal hydride hydrogen atom transfer conditions for alkene hydration^{44,45} led to tertiary alcohol formation and provided brassicene F (**33**) after silyl group removal.

In light of the intriguing bioactivity of the family members, access to additional derivatives with unnatural oxidation patterns would provide valuable compounds for future structure-activity relationship studies. During our initial attempts to convert **5** to **25**, it was found that the C6 position of **5** could be selectively oxidized with SeO_2 to provide an unnatural fusicoccane diterpenoid (Figure 3C). Additionally, screening of our P450_{BM3} library on **8** revealed that variant MERO1 FT is capable of oxidize primarily at C4 to afford yet another unnatural fusicoccane diterpenoid. Taken together, the late-stage synthetic tailoring of **8** through a combination of chemical and enzymatic C–H oxidations allowed us to divergently access not only five oxidized fusicoccanes, but also five rearranged family members and two unnatural derivatives in a concise fashion (less than 13 steps each), validating the design of our hybrid oxidative approach to this privileged terpenoid family.

Conclusion

This work describes the development of a modular chemoenzymatic synthesis of a wide range of oxidized and rearranged fusicoccanes—most of which were synthesized for the first time—from a common intermediate. Central to our approach is the combined use of efficient *de novo* skeletal construction to rapidly assemble the general fusicoccane tricycle and a hybrid oxidative approach to site-selectively hydroxylate various key positions on the carbocycle. Notably, one of the flagship family members, cotylenol was prepared in just 9 steps, marking the shortest synthesis of this natural product to date. Salient features of our approach include the use of a catalytic NHK reaction for the union of two cyclopentane fragments that also set the key quaternary center at C11, the development of a one-pot Prins cyclization/transannular hydride transfer to construct the central cyclooctene ring of the tricyclic scaffold, and the orchestration of late-stage hybrid oxidations to access various oxygenation patterns on the tricyclic core with minimal recourse to indirect synthetic manoeuvres. Moreover, we showed that the enzymatic oxidation component of the approach is highly tunable. Despite the sub-optimal conversion and selectivity of wild-type Bsc9, the combined use of homolog screening and directed evolution successfully yielded variants with

ca. two-fold improvement in activity and selectivity. Two engineered variants of P450_{BM3} provided complementary means to install further oxidations at C13 and C4, demonstrating the ability of this privileged catalyst family to accept 5/8/5 tricyclic ring system for the first time. Access to highly oxidized family members with our strategy in turn facilitates the design of a biomimetic skeletal reorganization by perceiving an alcohol group as a latent carbocation precursor to realize the first synthesis of several rearranged targets with unusual bridgehead double bonds. Cumulatively throughout this work, we show that almost any position on the fusicoccane skeleton can be oxidized by carefully tuning the order of reaction and judiciously choosing the oxidation catalysts/reagents. Looking ahead, the approach outlined here provides a general blueprint for accessing a large pool of valuable natural and unnatural fusicoccanes as potential probe molecules to study the 14-3-3 interactome and design new molecular glues to modulate 14-3-3 PPIs.

References

1. De Boer, A. H.; de Vries-van Leeuwen, I. J. Fusicoccanes: Diterpenes with surprising biological functions." *Trends Plant Sci.* **2012**, *17*, 360.
2. Ohkanda, J. Fusicoccin: A chemical modulator for 14-3-3 proteins. *Chem. Lett.* **2021**, *50*, 57.
3. Sengupta, A.; Liriano, J.; Bienkiewicz, E. A.; Miller, B. G.; Frederich, J. H. Probing the 14-3-3 isoform-specificity profile of protein-protein interactions stabilized by fusicoccin A. *ACS Omega* **2020**, *5*, 25029.
4. Molzan, M.; Kasper, S.; Röglin, L.; Skwarczynska, M.; Sassa, T.; Inoue, T.; Breitenbuecher, F.; Ohkanda, J.; Kato, N.; Schuler, M.; Ottmann, C. Stabilization of physical RAF/14-3-3 interaction by cotylenin A as treatment Strategy for RAS mutant cancers. *ACS Chem. Biol.* **2013**, *8*, 1869.
5. Zheng, D.; Han, L.; Qu, X.; Chen, X.; Zhong, J.; Bi, X.; Liu, J.; Jiang, Y.; Jiang, C.; Huang, X. Cytotoxic fusicoccane-type diterpenoids from *Streptomyces violascens* isolated from *Ailuropoda melanoleuca* feces. *J. Nat. Prod.* **2017**, *80*, 837.
6. Kim, S.; Shin, D.-S.; Lee, T.; Oh, K.-B. Periconicins, two new fusicoccane diterpenes produced by an endophytic fungus *Periconia* sp. with antibacterial activity. *J. Nat. Prod.* **2004**, *67*, 448.
7. Stevers, L. M.; Sijbesma, E.; Botta, M.; MacKintosh, C.; Obsil, T.; Landrieu, I.; Cau, Y.; Wilson, A. J.; Karawjczyk, A.; Eickhoff, J.; Davis, J.; Hann, M.; O'Mahony, G.; Doveston, R. G.; Brunsveld, L.; Ottman, C. Modulators of 14-3-3 protein-protein interactions. *J. Med. Chem.* **2018**, *61*, 3755.
8. Ikejiri, F.; Honma, Y.; Okada, T.; Urano, T.; Suzumiya, J. Cotylenin A and tyrosine kinase inhibitors synergistically inhibit the growth of chronic myeloid leukemia cells. *Int. J. Oncol.*, **2018**, *52*, 2061.
9. Kasukabe, T.; Okabe-Kado, J.; Honma, Y. Cotylenin A, a new differentiation inducer, and rapamycin cooperatively inhibit growth of cancer cells through induction of cyclin G2. *Cancer Sci.* **2008**, *99*, 1693.
10. Asahi, K.; Honma, Y.; Hazeki, K.; Sassa, T.; Kubohara, Y.; Sakurai, A.; Takahashi, N. Cotylenin A, a plant-growth regulator, induces the differentiation in murine and human myeloid leukemia cells. *Biochem. Biophys. Res. Commun.* **1997**, *238*, 758.
11. Anders, C.; Higuchi, Y.; Koschinsky, K.; Bartel, M.; Schumacher, B.; Thiel, P.; Nitta, H.; Preisig-Müller, R.; Schlichthöri, G.; Renigunta, V.; Ohkanda, J.; Daut, J.; Kato, N.;

- Ottmann, C. A semisynthetic fusicoccane stabilizes a protein-protein interaction and enhances the expression of K⁺ channels at the cell surface. *Chem. Biol.* **2013**, *20*, 583.
12. Hu, Z. et al. Fusicoccane-derived diterpenoids from *Alternaria brassicicola*: investigation of the structure-stability relationship and discovery of an IKK β inhibitor. *Org. Lett.* **2018**, *20*, 5198.
 13. Li, F. et al. Modified fusicoccane-type diterpenoids from *Alternaria brassicicola*. *J. Nat. Prod.* **2020**, *83*, 1931.
 14. Tang, Y. et al. Structural revisions of a class of natural products: scaffolds of aglycon analogues of fusicoccins and cotylenins isolated from fungi. *Angew. Chem. Int. Ed.* **2016**, *55*, 4069.
 15. Ohkanda, J.; Kusumoto, A.; Punzalan, L.; Masuda, R.; Wang, C.; Parvatkar, P.; Akase, D.; Aida, M.; Uesugi, M.; Higuchi, Y.; Kato, N. Structural effect of fusicoccin upon upregulation of 14-3-3 phospholigand interaction and cytotoxic activity. *Chem. Eur. J.* **2018**, *24*, 16066.
 16. Inoue, T.; Higuchi, Y.; Yoneyama, T.; Lin, B.; Nunomura, K.; Honma, Y.; Kato, N. Semisynthesis and biological evaluation of a cotylenin A mimic derived from fusicoccin A. *Bioorg. Med. Chem. Lett.* **2018**, *28*, 646.
 17. Ono, Y.; Minami, A.; Noike, M.; Higuchi, Y.; Toyomasu, T.; Sassa, T.; Kato, N.; Dairi T. Dioxygenases, key enzymes to determine the aglycon structures of fusicoccin and brassicicene, diterpene compounds produced by fungi. *J. Am. Chem. Soc.* **2011**, *133*, 2548.
 18. Kato, N.; Okamoto, H.; Takeshita, H. Total synthesis of optically active cotylenol, a fungal metabolite having a leaf growth activity. Intramolecular ene reaction for an eight-membered ring formation. *Tetrahedron* **1996**, *52*, 3921.
 19. Williams, D. R.; Robinson, L. A.; Nevill, C. R.; Reddy, J. P. Strategies for the synthesis of fusicoccanes by Nazarov reactions of dolabelladienones: total synthesis of (+)-fuscoauritone. *Angew. Chem. Int. Ed.* **2007**, *46*, 915.
 20. Uwamori, M.; Osada, R.; Sugiyama, R.; Nagatani, K.; Nakada, M. Enantioselective total synthesis of cotylenin A. *J. Am. Chem. Soc.* **2020**, *142*, 5556.
 21. Chen, B.; Wu, Q.; Xu, D.; Zhang, X.; Ding, Y.; Bao, S.; Zhang, X.; Wang, L.; Chen, Y. A two-phase approach to fusicoccane synthesis to uncover a compound that reduces tumorigenesis in pancreatic cancer cells. *Angew. Chem. Int. Ed.* **2022**, *61*, e202117476.
 22. Wang, Y.-Q.; Xu, K.; Min, L.; Li, C.-C. Asymmetric total syntheses of hypoestin A, albolic acid, and ceroplastol II. *J. Am. Chem. Soc.* **2022**, *144*, 10162.
 23. Sims, N. J.; Bonnet, W. C.; Lawson, D. M.; Wood, J. L. Enantioselective total synthesis of (+)-alterbrassicicene C. *J. Am. Chem. Soc.* **2023**, *145*, 37.
 24. Zhang, X.; Dong, L.-B.; Yang, L.-C.; Rudolf, J. D.; Shen, B.; Renata, H. Divergent Synthesis of Complex Diterpenes via a Hybrid Oxidative Approach. *Science* **2020**, *369*, 799.
 25. Tazawa, A.; Ye, Y.; Ozaki, T.; Liu, C.; Ogasawara, Y.; Dairi, T.; Higuchi, Y.; Kato, N.; Gomi, K.; Minami, A.; Oikawa, H. Total biosynthesis of brassicicenes: Identification of a key enzyme for skeletal diversification. *Org. Lett.* **2018**, *20*, 6178.
 26. Chakrabarty, S.; Wang, Y.; Perkins, J. C.; Narayan, A. R. H. Scalable biocatalytic C–H oxyfunctionalization reactions. *Chem. Soc. Rev.* **2020**, *49*, 8137.
 27. Fasan, R. Tuning P450 enzymes as oxidation catalysts. *ACS Catal.* **2012**, *2*, 647.

28. Lange, G. L.; Neider, E. E.; Orrom, W. J.; Wallace, D. J. Synthesis of the spirosesquiterpene (-)-acorenone and related cyclopentanoid monoterpenes. *Can. J. Chem.* **1978**, *56*, 1628.
29. Uroos, M.; Lewis, W.; Blake, A. J.; Hayes, C. J. Total synthesis of (+)-cymbodiacetal: a re-evaluation of the biomimetic route. *J. Org. Chem.* **2010**, *75*, 8465.
30. Fürstner, A.; Shi, N. Nozaki–Hiyama–Kishi reactions catalytic in chromium. *J. Am. Chem. Soc.* **1996**, *118*, 12349.
31. Kilpatrick, M.; Luborsky, F. E. The conductance and vapor pressure of boron trifluoride in anhydrous hydrofluoric acid. *J. Am. Chem. Soc.* **1954**, *76*, 5865.
32. Vedejs, E.; Engler, D. A.; Telschow, J. E. Transition-metal peroxide reactions. Synthesis of α -hydroxycarbonyl compounds from enolates. *J. Org. Chem.* **1978**, *43*, 188.
33. Baek, M.; DiMaio, F.; Anishchenko, I.; Dauparas, J.; Ovchinnikov, S.; Lee, G. R.; Wang, J.; Cong, Q.; Kinch, L. N.; Schaeffer, R. D.; Millán, C.; Park, H.; Adams, C.; Glassman, C. R.; DeGiovanni, A.; Pereira, J. H.; Rodrigues, A. V.; van Dijk, A. A.; Ebrecht, A. C.; Opperman, D. J.; Sagmeister, T.; Buhlheller, C.; Pavkov-Keller, T.; Rathinaswamy, M. K.; Dalwadi, U.; Yip, C. K.; Burke, J. E.; Garcia, K. C.; Grishin, N. V.; Adams, P. D.; Read, R. J.; Baker, D. Accurate prediction of protein structures and interactions using a three-track neural network. *Science*, **2021**, *373*, 871.
34. Zallot, R.; Oberg, N.; Gerlt, J. A. The EFI web resource for genomic enzymology tools: Leveraging protein, genome, and metagenome databases to discover novel enzymes and metabolic pathways. *Biochemistry* **2019**, *58*, 4169.
35. Jiang, Y.; Renata, H. Finding superior biocatalysts via homolog screening. *Chem Catal.* **2022**, *2*, 2471.
36. Kille, S.; Acevedo-Rocha, C. G.; Parra, L. P.; Zhang, Z.-G.; Opperman, D. J.; Reetz, M. T.; Acevedo, J. P. Reducing codon redundancy and screening effort of combinatorial protein libraries created by saturation mutagenesis. *ACS Synth. Biol.* **2013**, *2*, 83.
37. Li, F.; Deng, H.; Renata, H. Remote B-ring oxidation of sclareol with an engineered P450 facilitates divergent access to complex terpenoids. *J. Am. Chem. Soc.* **2022**, *144*, 7616.
38. Li, J.; Li, F.; King-Smith, E.; Renata, H. Merging Chemoenzymatic and Radical-Based Retrosynthetic Logic for Rapid and Modular Synthesis of Oxidized Meroterpenoids. *Nature Chem.* **2020**, *12*, 173.
39. Li, F.; Renata, H. A Chiral-Pool-Based Strategy to Access Trans-Syn-Fused Drimane Meroterpenoids: Chemoenzymatic Total Syntheses of Polysin, N-Acetyl-Polyveoline and the Chrodrimanins. *J. Am. Chem. Soc.* **2021**, *143*, 18280.
40. Li, J.; Chen, F.; Renata, H. Concise Chemoenzymatic Synthesis of Gedunin. *J. Am. Chem. Soc.* **2022**, *144*, 19238.
41. Yu, J.-Q.; Corey, E. J. Diverse pathways for the palladium(II)-mediated oxidation of olefins by tert-butylhydroperoxide. *Org. Lett.* **2002**, *4*, 2727.
42. Ting, C. P.; Maimone, T. J. Total synthesis of hyperforin. *J. Am. Chem. Soc.* **2015**, *137*, 10516.
43. Ishiyama, S.; Mukaiyama, T. Novel method for the preparation of triethylsilyl peroxides from olefins by the reaction with molecular oxygen and triethylsilane catalyzed by bis(1,3-diketonato)cobalt(II) *Chem. Lett.* **1989**, *18*, 573.
44. Crossley, S. W. M.; Obradors, C.; Martinez, R. M.; Shenvi, R. A. Mn-, Fe-, and Co-catalyzed radical hydrofunctionalizations of olefins. *Chem. Rev.* **2016**, *116*, 8912.

45. Isayama, S.; Mukaiyama, T. A new method for preparation of alcohols from olefins with molecular oxygen and phenylsilane by the use of bis(acetylacetonato)cobalt(II). *Chem. Lett.* **1989**, *18*, 1071.

Acknowledgments: We acknowledge funding from the National Institutes of Health Grant R35128895 (H.R.), the Cancer Prevention and Research Institute of Texas (CPRIT) grant RR220087, and the Sloan Foundation. We are grateful to the Shen and Bannister labs at the Wertheim UF-Scripps Institute for Biomedical Innovation and Technology, and to the Nicolaou, Kürti and Xiao labs and the Shared Equipment Authority at Rice University for generous access to their reagents and instrumentation. H.R. is a CPRIT scholar in cancer research.

Funding:

National Institutes of Health grant R35GM128895 (HR)

Cancer Prevention and Research Institute of Texas (CPRIT) grant RR220087 (HR)

Sloan Foundation (HR)

Author contributions: Y.J. and H.R. conceived the work. Y.J. and H.R. designed all the experiments described in the manuscript. H.R. wrote the manuscript; Y.J. assisted in writing and editing the manuscript.

Competing Interests: The authors have applied for a provisional patent for this work. A portion of the present manuscript is drawn from a previous preprint from our laboratory: <https://chemrxiv.org/engage/chemrxiv/article-details/6332fee8114b7e5fe81f55df>.

Data and materials availability: All data is available in the main text or the supplementary materials.

Supplementary Materials

Materials and methods

Tables S1 to S25